CONTROL OF DYNAMICAL STATES IN A NETWORK: FIRING DEATH AND MULTISTABILITY

Marzena Ciszak
CNR-Istituto Nazionale di Ottica
Italy
marzena.ciszak@ino.it

Stefano Euzzor
CNR-Istituto Nazionale di Ottica
Italy
stefano.euzzor@ino.it

F. Tito Arecchi
CNR-Istituto Nazionale di Ottica
Italy
tito.arecchi@ino.it

Riccardo Meucci
CNR-Istituto Nazionale di Ottica
Italy
riccardo.meucci@ino.it

Abstract

We show that the chaotically spiking neurons coupled in a ring configuration changes their internal dynamics to subthreshold oscillations, the phenomenon referred to as firing death. These dynamical changes are observed below the critical coupling strength at which the transition to full chaotic synchronization occurs. We find various dynamical regimes in the subthreshold oscillations, namely, regular, quasi-periodic and chaotic states. We show numerically that these dynamical states may coexist with large amplitude spiking regimes and that this coexistence is characterized by riddled basins of attraction. Moreover, we show that under a particular coupling configuration, the neural network exhibits bistability between two configurations of clusters. Each cluster composed of two neurons undergoes independent chaotic spiking dynamics. As an appropriate external perturbation is applied to the system, the network undergoes changes in the clusters configuration, involving different neurons at each time. We hypothesize that the winning cluster of neurons, responsible for perception, is that exhibiting higher mean frequency. The clusters features may contribute to an increase of local field potential in the neural network. The reported results are obtained for neurons implemented in the electronic circuits as well as for the model equations.

Key words

neural network; chaotic spiking; network topology; bistable attractors; firing death; synchronization

1 Introduction

In the case of spatially extended systems, the dynamical regimes of the single nodes and global states are influenced by the intercellular interactions through the different types of coupling. For example, the chaotic spiking behaviour in the two-dimensional oscillatory FHN can be induced by coupling systems in a network [Yanagita, Ichinomiya and Oyama, 2005]. It has been shown that coupling can also induce a quasi-periodic motion [Sano and Sawada, 1983; Van Buskirk and Jeffries, 1985]. The transition from regular periodic dynamics to quasi-periodicity may occur through a Neimark-Sacker [Gumowski and Mira, 1980] or border-collision [Zhusubaliyeva et al, 2006] bifurcations. These bifurcations lead to a quasi-periodic route to chaos (Ruelle-Takens scenario). The emergence of complex firing patterns in a neural network may be induced not only by coupling but also by the presence of delays [Popovych, Yanchuk and Tass, 2011]. Despite the dynamical changes and creation of multistable states, above a certain coupling strength, the systems eventually reach full synchronization.

On the other hand, the coupling may reduce the complexity of the network leading to the so-called *oscillation* or *amplitude death* where the dynamics of each subsystem ends up in a stable fixed point through the Hopf or saddle-node bifurcations. It was shown in [Aronson, Ermentrout, and Kopell, 1990], that in a pair of weakly nonlinear oscillators, the coupling strength causes the system to stop oscillating, and the rest state at zero, stabilized by the interaction, is the only stable solution. The amplitude death may be eliminated by introducing the disorder in the form of random deviations from a linear trend of frequencies in an array of diffusively coupled limit-cycle oscillators [Rubchinsky and Sushchik, 2000]. Such approach weakens considerably desynchronization-induced oscillator death and, as a result, increase oscillation intensity substantially. The amplitude death was also demonstrated to be induced not only by coupling but also by time-delay [Ramana Reddy, Sen and Johnston, 2000]. It was shown

in two coupled nonlinear electronic circuits that are individually capable of exhibiting limit-cycle oscillations. Other experimental observations regarded a pair of thermo-optical oscillators linearly coupled by heat transfer [Herrero et al, 2000]. It was demonstrated that the death phenomenon occurs because the coupling displaces the Hopf bifurcation point.

A similar phenomenon takes place in the systems with two time scales. The large coupling may lead to the so-called *firing* or *spike death* in a network, where the coupled neurons enter the subthreshold oscillation regime. It was demonstrated [Verhulst and Abadi, 2005; Hennig and Schimansky-Geier, 2007], that coupling induces deformation of the slow manifolds leading to suppression of large amplitude oscillations (canards). In [Hennig and Schimansky-Geier, 2007], two coupled FHN have been studied theoretically examining their response to heterogeneous external parametrical inputs applied to the slow variable. The firing death was shown to occur at large coupling strengths and be caused by a coupling-induced modification of the slow manifold leading to the increase of the excitation threshold.

Under particular coupling configuration the network exhibits multistable states. Multistability, in particular bistability has been subject to intense study due to the possible biological applications. For example, the first proposal that the bistable transitions may play a role in the ambiguous perception, was presented by Haken [Haken, 1994]. The detailed models implementing the idea have been analyzed through considering the switching processes between the attractors of a network under the effect of noise [Moreno-Bote, Rinzel and Rubin, 2007]. These approaches reproduce well all the characteristics found in experimental data. However, the existence of a high complexity in neural responses gives a cue about the deterministic rather than stochastic functioning of the brain units. This of course does not exclude the existence of noisy fluctuations but restricts its action on decision making processes which are not random but deterministic.

Here we examine a network of four FHN electronic neurons coupled in a ring configuration subjected to homogenous external inputs in the fast variables [Ciszak at al, 2013]. We show that the firing death may occur at small coupling strengths, i.e. before the full synchronization establishes. The occurrence of this phenomenon at small coupling strengths is possible because the slow manifold is modified by both, the external forcing and coupling. As the coupling strength is slowly increased, the firing is replaced by subthreshold oscillations exhibiting regular, quasi-periodic (through the Neimark-Sacker bifurcation) or chaotic oscillations. We show numerically that the subthreshold oscillations may coexist with the large amplitude spiking and that their coexistence is characterized by the riddled basins of attraction. Moreover, we consider FHN systems with inhibitory and excitatory couplings [Ciszak at al, 2012]. We show that in a certain range of the coupling parameters, such a network undergoes bistable behaviour. Considering four interacting neurons we observe the emergence of two clusters with independent chaotic dynamics. The crucial difference between the clusters is the frequency of chaotic spiking. One cluster dominates over the other through the higher mean frequency and thus it contributes to higher Local Field Potential (LFP). This may be a possible mechanism of effective competition between the two perceptual choices.

2 Experimental setup and the model

The circuit implementing the FHN is made of commercial semiconductor devices. A network of four FHN has been realized on printed circuit, planned by using OrCad. The electronic network consists of a nearest neighbor closed loop coupling scheme, as shown in Fig. 1. The scheme for the electronic circuit reproducing each FHN is shown in Fig. 2 (a), while that for the coupling implementation is shown in Fig. 2 (b). The equations describing each FHN circuit are:

$$\begin{aligned}\dot{X}_i &= \frac{1}{R_1 C_1}\left(X_i - X_i^3/3 - Y_i + V_d + \alpha \Delta X_i\right)\\ \dot{Y}_i &= \frac{1}{R_1 C_2}\left(\frac{R_1}{R_3}V_b - \frac{R_1}{R_2}Y_i + X_i\right)\end{aligned} \tag{1}$$

where $i = 1, ..., 4$ indicates the nodes in the network, V_d is the driving signal $A\sin(2\pi\nu t)$ and V_b is a bias voltage. The constant parameters are $R_1C_1 = 1$, $C_1/C_2 = 1/(R_1C_2) = 0.08$, $R_1/R_2 = 0.8$ and $R_1/R_3 = 0.7$, where R stands for resistance and C for capacitor. The nonlinearity X^3 is realized by means of analogue multipliers. The temporal scales of the systems are controlled by R_1 and C_1 for the X variable and by R_1 and C_2 for the Y variable. The coupling strength $\alpha = R_e/R$ is determined by a suitable value of a variable resistor. The coupling term ΔX_i is composed with differential amplifiers which allow to subtract the signals coming from the neighboring nodes X_{i-1} and X_{i+1} and the feedback signal X_i.

On the other side, the model equations for the driven FHN are the following:

$$\begin{aligned}\dot{x}_i &= x_i - x_i^3/3 - y_i + F + \alpha \Delta x_i\\ \dot{y}_i &= \gamma(a - by_i + x_i)\end{aligned} \tag{2}$$

where x_i is the fast variable, y_i is the recovery variable and $F = A\sin(2\pi\nu t)$ is an external driving term with amplitude A and frequency $\nu = 1/T$. We consider fixed parameters: $\gamma = 0.08$, $a = 0.7$, $b = 0.8$, and for the external forcing: $A = 0.485$ and $T = 0.636$. Parameter α is the coupling strength. Equation 2 is transformed to the three-variable set of equations by intro-

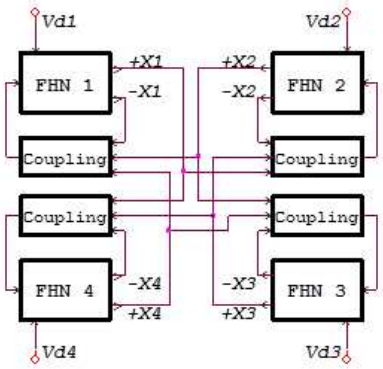

Figure 1. Scheme for the network of four FHN.

ducing a new variable $z_i = 2\pi\nu t = \omega t$, as follows:

$$\begin{aligned} \dot{x}_i &= x_i - x_i^3/3 - y_i + A\sin z_i + \alpha\Delta x_i \\ \dot{y}_i &= \gamma(a - by_i + x_i) \\ \dot{z}_i &= \omega. \end{aligned} \tag{3}$$

Δx_i (as well as ΔX_i in the case of the experiment) is the coupling term describing the nearest neighbour configuration:

$$\Delta x_i = (x_{i-1} + x_{i+1} - 2x_i) \tag{4}$$

for $i = 1, ..., 4$ and periodic boundary conditions.

Despite of the ring configuration with nearest-neighbour configuration we consider also asymmetric coupling defined as follows:

$$\begin{aligned} \Delta x_{1,3} &= x_4 - x_2 \\ \Delta x_{2,4} &= x_1 - x_3. \end{aligned} \tag{5}$$

where the nodes receive both, excitatory and inhibitory signals (see Fig. 3).

3 Results

3.1 Dynamical regimes induced by coupling

The experimental implementation of identical oscillators is very hard, and the parameter mismatches of unknown magnitude usually arises. A reasonable mismatch in the control parameter can be estimated to be of order of 10^{-2}. However, in the experimental system we are dealing not only with parameter mismatch but also with an idealized nonlinear function (assumed for simplicity and without loss of generality to be cubic). It is likely that such a mismatch in the description of the nonlinear terms (a multi-valued function, though not strictly cubic) is much more relevant than the accuracy in determining the exact values of the control parameters. For the sake of simplicity, here we consider the mismatch only in one control parameter (we choose

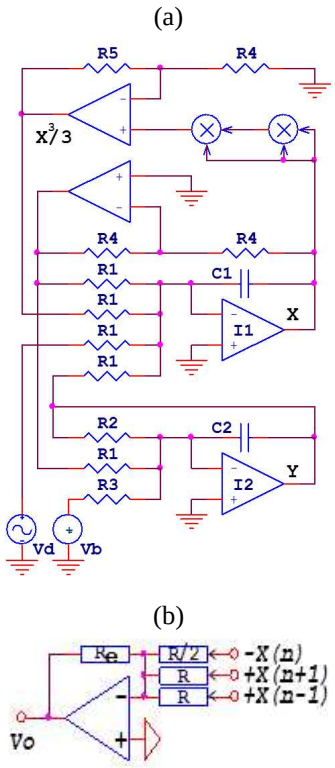

Figure 2. Schemes of (a) the electronic circuit implementing driven FHN and (b) the electronic coupling.

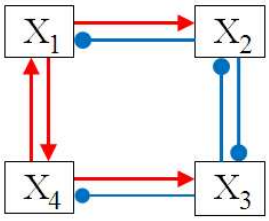

Figure 3. Scheme of the neural network with inhibitory (circles) and excitatory (arrows) connections that produces bistable patterns.

parameter $a \rightarrow a_i$) and find the similar sequences of regimes observed experimentally.

In a certain parameter range we observe firing death where the large amplitude oscillations are suppressed giving rise the small amplitude subthreshold oscillations (see Fig. 4 (b)). The firing death is also observed for identical systems (Fig. 4 (a)) as well as for systems with much larger mismatches, demonstrating that this dynamical transition is due to the coupling and not system's diversities.

The presence of the external forcing in the fast variable induces the spike suppression at much smaller coupling strengths compared with the case when it is applied to the slow variable. As the coupling strength is increased, the critical point at which the canard explosion takes place is modified. This is due to the fact, that at large α, when fully synchronized state is reached, the difference variables Δx_i go to zero and thus after the

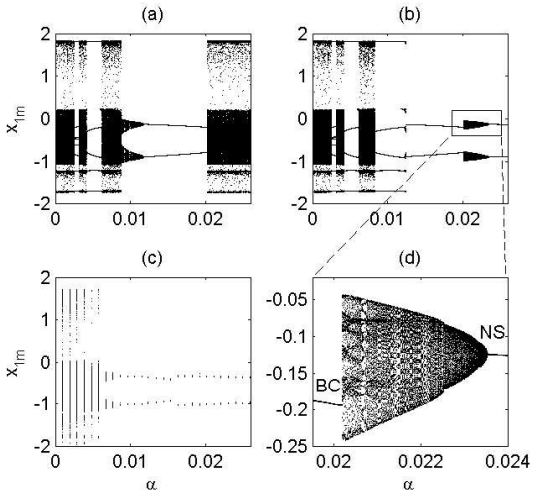

Figure 4. Bifurcation diagrams for identical model systems (a), and for model systems with slight mismatches (b) and the experiment (c). In (d) the details of the region with quasi-periodic route to chaos are shown, marking Neimark-Sacker (NS) and boundary crisis (BC) bifurcations. The parameter α is increased as shown in Fig. **??** (e).

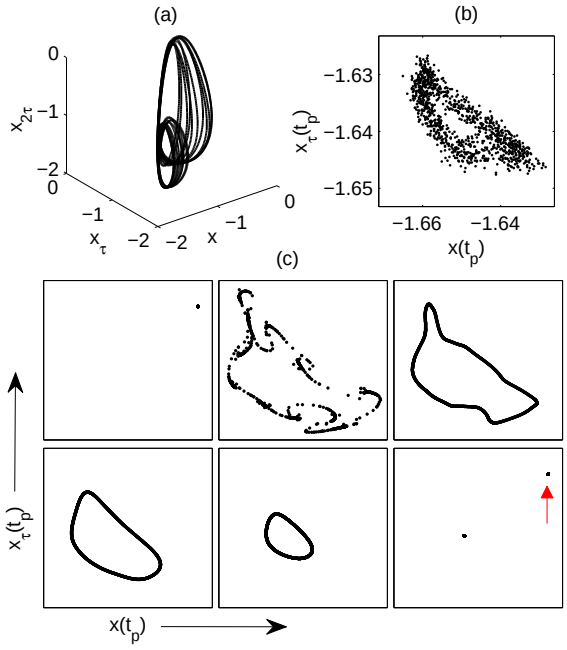

Figure 5. (a) Reconstructed phase space and (b) corresponding Poincaré cross-section obtained from experiment for $\alpha = 0.03$, $A = 899$mVpp and $\omega = 400$Hz. (c) Poincaré cross-section in the region where the quasi-periodicity route to chaos is observed. The cross-sections are taken for the following coupling parameters: $\alpha = \{0.02, 0.02005, 0.021, 0.0215, 0.023, 0.024\}$. The coupling parameter is increased gradually from 0.02 to 0.024. The small arrow in the last panel marks the orbit before the bifurcation sequence took place (orbit from the first panel).

initial transient the coupling term reaches small values and does not change any longer the internal dynamics of the system.

The subthreshold oscillations undergo the transitions from the regular, to quasi-periodic and chaotic. At approximately $\alpha = 0.024$ we observe the Neimark-Sacker bifurcation, where the transition from a periodic to quasi-periodic subthreshold orbit occurs. Successively, the quasi-periodicity route to chaos is observed (see Fig. 4 (d)). Here, this scenario is related with the change in shape of the subthreshold periodic orbit. At the end of the bifurcation sequence, the chaotic attractor suddenly disappears through a boundary crisis, giving rise to a new periodic orbit. Both orbits, before and after the bifurcation cascade, have the same frequency of oscillations.

The ratio $w = \Omega/\omega$ defines the winding number. It describes the number of times the trajectory winds around the small cross-section of the torus (described by Ω, that is the frequency of the system) after going once around the large circumference of torus (described by ω, that is the frequency of driving). If the frequencies are commensurate (w is rational), then the motion is periodic, otherwise (if w is irrational), the trajectory fills the whole toroidal surface and contributes to quasi-periodic motion. At the certain coupling values a winding number becomes irrational that consequently leads to quasi-periodic solutions. In order to detect the quasi-periodic motion we take a Poincaré section of a reconstructed attractor, both experimentally (Fig. 5 (a-b)) and in the model (Fig. 5 (c)). We reconstruct the phase space through the embedding technique with $d = 2$ and take the values of $x(t)$ and $x(t+\tau)$ at times that correspond to a period $T = 2\pi/\omega$ of external forcing. The subthreshold oscillations are composed of subharmonics of order $n = 2$, thus have period $2T$, where T is the period of the fundamental solution (and corresponds to the period of forcing). In a certain range of parameter α each subharmonic undergoes the quasi-periodic route to chaos. As the bifurcation cascade finishes, the subharmonics remain with period $2T$, but change the amplitude of oscillations (see the last panel of Fig. 5 (c)).

3.2 Network multistability

The system exhibits multistable states throughout a wide range of coupling parameter α, well seen as α is slowly increased or decreased. We identified various coexistent states including the regular subthreshold oscillations and large amplitude regular spiking, regular and chaotic subthreshold oscillations, large lower and higher amplitude regular oscillations as well as large amplitude regular and chaotic spiking. Here we analyze in detail only one case (at $\alpha = 0.035$), namely the coexistence of the regular subthreshold oscillations and spiking.

The basin of attraction of the observed coexistent states exhibits riddling (see Fig. 6 (a)). Riddling refers to the situation in which every point in the basin of attraction of attractor A has pieces of the basin of attraction of attractor B arbitrarily nearby. Thus the exis-

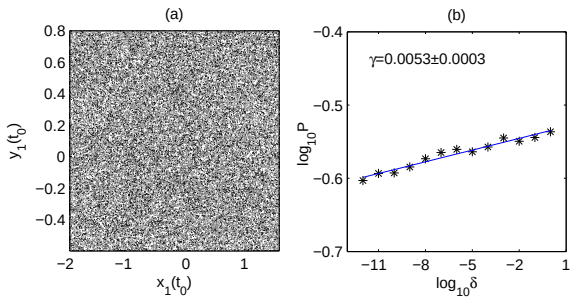

Figure 6. (a) Basin of attraction for the coupled systems with slight mismatches. Black and gray colors mark small and large amplitude oscillations, respectively. (b) The uncertainty exponent calculated for (a).

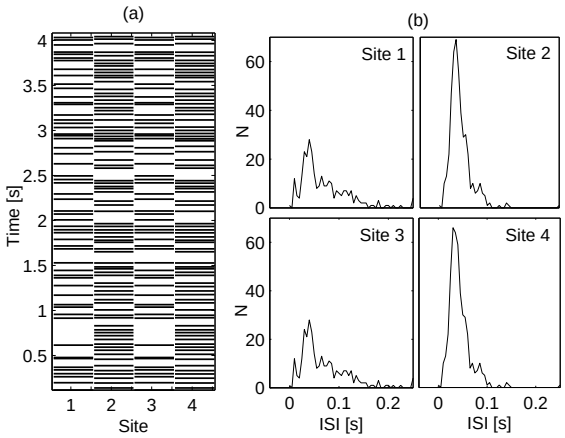

Figure 7. (a) The raster plot for four coupled FHN systems obtained from the experiment. Each horizontal line marks the appearance of a spike in time at each site. (b) Distribution of ISI calculated from the time series corresponding to the raster plot shown in (a).

tence of riddled basins of attraction compromises the predictability of the final state of the system [Kapitaniak, 1996]. The riddled basin can be characterized in terms of the uncertainty exponent γ [Grebogi et al, 1983]. We calculate the exponent γ as described in [Guan, Lai and Wei, 2005]. First, we choose randomly a phase point r_0. Then we define another phase point $r_0' = r_0 + \delta$, where δ is a small separation from the initial point r_0. Using these two initial conditions we determine whether the final states of the system are different. For a given perturbation δ, we repeat the simulations by choosing randomly many different initial conditions and estimate the fraction M from all realizations N that leads to different states. We fix the initial parameters for three FHN oscillators, while we randomly change those of the remaining one. Using these data, we calculate the probability $P(\delta) = M/N$ and from the assumption that $P(\delta) \sim \delta^{\gamma}$, we estimate the uncertainty exponent γ. In Fig. 6 (b) we plot $\log_{10}(P)$ versus $\log_{10}(\delta)$, with the uncertainty exponent γ that is the slope of the straight line. We have evaluated the system numerically approximately 3.5×10^5 times for each selected δ. Using linear fit we get the approximate value of the uncertainty exponent to be $\gamma = 0.0053 \pm 3 \times 10^{-4}$, which is considerably smaller than typical values usually obtained for non-riddled basins of attraction. We note, that also for other coexistent states, the basins of attraction exhibit riddling.

Let us now consider the coupling configuration defined in Eq. 5 and shown graphically in Fig. 3. We observe the formation of synchronized clusters, that is determined by asymmetric inhibitory and excitatory connections in the network. More precisely, the network is composed of two excitatory and two inhibitory neurons. The bistable switching occurs for the pairs of exhibitory-inhibitory neurons. The crucial difference between the two formed clusters is the frequency of chaotic spiking. In Fig. 7 (a) we report the raster plot that shows spiking times of each node in the experimentally implemented network. The formation of two clusters is observed, each characterized by different inter-spike interval (ISI) distributions as seen in Fig. 7 (b). One cluster dominates over the other through the higher mean frequency and thus contributes to higher LFP.

4 Discussion

The dynamical regimes, that the network has to pass through in order to get synchronized, are well visible when the coupling strength is varied slowly and linearly. As the coupling is varied fast to higher values, all dynamical details which we have identified here are lost. The suppression of spiking or emergence of periodic spiking during transition to synchronization at slowly varied coupling strength is an interesting point, suggesting that the coupling strength destroys the initial state completely during the transient, and recovers it through the well-determined bifurcation cascade when full synchronization is reached. This phenomenon may be of crucial importance in biological complex systems, for instance, during the spike time depending plasticity (STDP) [Markram, 1997] that controls neural connections, where the synaptic strengths are increased or decreased due to potentiation or depotentiation phenomena, respectively. It could serve as a control tool in the brains' neural network obeying the synaptic plasticity rule and could give rise to fast transitions from quiescence to activity and *vice versa*. In fact, it has been shown that STDP may lead the network to various dynamical states (including chaotic bursting). Other example to mention is the possible role of the coupling in the emergence of cardiac deceases. The weak coupling between cardiac cells, may lead to oscillation death of the given subnetwork what may induce the malfunctioning of the entire organ.

We have shown, both numerically and experimentally, that a slow variation of the coupling in chaotically spiking neurons leads to firing death phenomena where all neurons set to subthreshold oscilla-

tions state. This occurs below the critical coupling strength at which the full chaotic synchronization establishes. The subthreshold oscillations may be regular, quasi-periodic (through Neimark-Sacker bifurcation) or chaotic. Moreover, we have found that these oscillations can coexist with large amplitude spiking and that this coexistence is characterized by riddled basins of attraction. We have demonstrated that the emergence of firing death at small coupling strength depends strongly on the complexity of a single node, and in particular, on the form of the fast variables.

Finally, we proposed a simple network composed of chaos generating systems to model perceptual bistability. We considered four chaotic FHN systems coupled through the inhibitory and excitatory connections. We observed the emergence of two synchronized clusters that undergo independent chaotic dynamics characterized by different mean frequency of spiking. Due to these differences one cluster dominates over the other and contributes stronger to LFP leading consequently to the strengthening of a given perceptual state. This may be a possible mechanism of effective competition between the two perceptual choices.

Acknowledgements

Work partly supported by Ente Cassa di Risparmio di Firenze. MC and RM acknowledge Regione Toscana for financial support.

References

Ciszak, M., Euzzor, S., Arecchi, F. T., and Meucci, R. (2013) Experimental study of firing death in a network of chaotic FitzHugh-Nagumo neurons. *Phys. Rev. E*, **87**, pp. 022919.

Ciszak, M., Euzzor, S., Farini, A., Arecchi, F. T., and Meucci, R. (2013) Modeling bistable perception with a network of chaotic neurons. *Cybernetics and Physics*, **1**(3), pp. 165.

Yanagita, T., Ichinomiya, T. and Oyama, Y. (2005) Pair of excitable FitzHugh-Nagumo elements: Synchronization, multistability, and chaos. *Phys. Rev. E*, **72**, pp. 056218.

Sano, M. and Sawada, Y. (1983) Transition from quasiperiodicity to chaos in a system of coupled nonlinear oscillators. *Physics Letters*, **97**A, pp. 73.

Van Buskirk, R. and Jeffries, C. (1985) Observation of chaotic dynamics of coupled nonlinear oscillators. *Phys. Rev. A*, **31**, pp. 3332.

Gumowski, I. and Mira, C. (1980). *Recurrence and Discrete Dynamic Systems*. Lecture Notes in Mathematics Vol. 809, Springer, Berlin.

Zhusubaliyeva, Z. T., Mosekilde, E., Maity, S., Mohanan, S., and Banerjeec, S. (2006) Border collision route to quasiperiodicity: Numerical investigation and experimental confirmation. *Chaos*, **16**, pp. 023122.

Popovych, O. V., Yanchuk, S., and Tass, P. A. (2011) Delay- and coupling-induced firing patterns in oscillatory neural loops. *Phys. Rev. Lett.*, **107**, pp. 228102.

Aronson, D. G., Ermentrout, G. B., and Kopell, N. (1990) Amplitude response of coupled oscillators. *Physica D*, **41**, pp. 403.

Rubchinsky, L., and Sushchik, M. (2000) Disorder can eliminate oscillator death. *Phys. Rev. E*, **62**, pp. 6440.

Ramana Reddy, D. V., Sen, A., and Johnston, G. L. (2000) Experimental evidence of time-delay-induced death in coupled limit-cycle oscillators. *Phys. Rev. Lett.*, **85**, pp. 3381.

Herrero, R., Figueras, M., Rius, J., Pi, F., and Orriols, G. (2000) Experimental observation of the amplitude death effect in two coupled nonlinear oscillators. *Phys. Rev. Lett.*, **84**, pp. 5312.

Verhulst, F., and Abadi, A. (2005) Autoparametric resonance of relaxation oscillations. *ZAMM - Z. Angew. Math. Mech.*, **85**, pp. 122.

Hennig, D., and Schimansky-Geier, L. (2007) Synchronization and firing death in the dynamics of two interacting excitable units with heterogeneous signals. *Phys. Rev. E*, **76**, pp. 026208.

Haken, H. (1994) A brain model for vision in terms of synergetics. *J. Theor. Biol.*, **171**, pp. 75-85.

Moreno-Bote, R., Rinzel, J. and Rubin, N. (2007) Noise-Induced Alternations in an Attractor Network Model of Perceptual Bistability. *J. Neurophysiol.*, **98**, pp. 1125–1139.

Kapitaniak, T. (1996) Uncertainty in coupled chaotic systems: Locally intermingled basins of attraction. *Phys. Rev. E*, **53**, pp. 6555.

Grebogi, C., McDonald, S. W., Ott, E., and Yorke, J. A. (1983) Final state sensitivity: An obstruction to predictability. *Phys. Lett.*, **99**A, pp. 415.

Guan, S., Lai, C.-H., and Wei, G. W. (2005) Bistable chaos without symmetry in generalized synchronization. *Phys. Rev. E*, **71**, pp. 036209.

Markram, H., Lubke, J., Frotscher, M., and Sakmann, B. (1997) Regulation of synaptic efficacy by coincidence of postsynaptic APs and EPSPs. *Science*, **275**, pp. 213.